EUROPEAN ORGANIZATION FOR NUCLEAR RESEARCH

CERN-EP/84-73
June 22nd, 1984

NEUTRAL D MESON PROPERTIES IN 360 GEV/c π^-p INTERACTIONS

LEBC-EHS COLLABORATION

Aachen[1]-Bombay[2]-Brussels[3]-CERN[4]-Collège de France[5]
Genova[6]-Japan Universities[7] (Chuo University, Hiroshima University, Tokyo Metropolitan University, Tokyo Univ. of Agriculture and Technology)
Liverpool[8]-Madrid[9]-Mons[10]-Oxford[11]-Padova[12]-Paris[13]-Roma[14]
Rutherford[15]-Rutgers[16]-Serpukhov[17]-Stockholm[18]-Strasbourg[19]
Tennessee[20]-Torino[21]-Trieste[22]-Vienna[23] Collaboration

M. Aguilar-Benitez[9], W.W. Allison[11] P. Bagnaia[14], J.F. Baland[10], S. Banerjee[2], W. Bartl[23], P. Beillère[5], G. Bertrand-Coremans[3], A. Bettini[12], G. Borreani[21], R. Bizzarri[14], H. Briand[13], R. Brun[4], W.M. Bugg[20], C. Caso[6], B. Castano[9], E. Castelli[22], G. Ciapetti[14], P. Checchia[12], P. Chliapnikov[17], S. Colwill[11], R. Contri[6], D. Crennell[15], M. Cresti[12], A. De Angelis[12], L. De Billy[13], Ch. Defoix[5], M. Deutschmann[1], E. Di Capua[14], R. Di Marco[16], J. Dolbeau[5], J. Dumarchez[4], B. Epp[23], S. Falciano[14], C. Fernandez[4], C. Fisher[15], Yu. Fisjak[17], F. Fontanelli[6], J.R. Fry[8], S. Ganguli[2], U. Gasparini[12], S. Gentile[14], F. Grard[10], A. Gurtu[2], T. Handler[20], R. Hamatsu[7], E.L. Hart[20], L. Haupt[18], S. Hellman[18], J. Hernandez[4], Ph. Herquet[10], A. Hervé[4], S.O. Holmgren[18], M.A. Houlden[8], J. Hrubec[23], Ph. Hughes[15], D. Huss[4], M. Iori[14], E. Jegham[19], E. Johansson[4], I. Kita[7], E. Kistenev[17], S. Kitamura[7], V. Knjasev[17], P. Ladron de Guevara[9], M. Laloum[5], J. Lemonne[3], H. Leutz[4], P. Lutz[5], M. MacDermott[15], P.K. Malhotra[2], F. Marchetto[21], G. Marel[14], J.Cl. Marin[4], F. Marzano[14], M. Mazzucato[12], A. Michalon[19], M.E. Michalon-Mentzer[19], T. Moa[18], L. Montanet[4], A. Moreton[8], G. Neuhofer[23], H. Nguyen[13], V. Nikolaienko[17], S. Nilsson[18], H. Nowak[4], N. Oshima[7], G. Otter[1], G.D. Patel[8], M. Pernicka[23], L. Peruzzo[12], P. Pilette[10], C. Pinori[12], G. Piredda[14], R. Plano[16], A. Poppleton[4], P. Poropat[22], R. Raghavan[2], S. Reucroft[4], J. Richardson[4], S. Rinaudo[21], K. Roberts[8], H. Rohringer[23], G. Sartori[12], H. Schlütter[1], J. Schmiedmayer[23], R. Schulte[1], W. Struczinski[1], M. Schouten[4], B. Sellden[18], M. Sessa[22], K. Shankar[2], P. Stamer[16], K.M. Stopchenko[17], A. Subramanian[2], K. Sudhakar[2], S. Squarcia[6], M.Cl. Touboul[4], U. Trevisan[6], C. Troncon[22], T. Tsurugai[7], L. Ventura[12], P. Vilain[3], E.V. Vlasov[17], B. Vonck[3], B.M. Whyman[8], J. Wickens[3], C. Willmott[9], P. Wright[4], T. Yamagata[7], L. Zanello[14], P. Zotto[12], G. Zumerle[12].

ABSTRACT

Based on a sample of 22 four-prong $D^0/\bar{D}^0$ decays produced in hydrogen by 360 GeV/c π^-, we present the following new results: mean lifetime $\tau = \left(3.5 \pm {}^{1.0}_{0.9}\right) \times 10^{-13}$ s; production cross section for $x_F > 0.0$, $\sigma = (10.3 \pm 3.5)$ μb; the $D \to K^{\pm}\pi^{\mp}\pi^+\pi^-$ branching ratio $= (7.1 \pm 2.5)\%$.

Submitted to Physics Letters B

In this paper we discuss the properties of the charm D^0 meson(*) produced by the interactions of 360 GeV/c π^- in liquid hydrogen. Data were collected for experiment NA27 in the North Area of the CERN SPS using the Rapid Cycling Lexan Bubble Chamber LEBC [1] and the European Hybrid Spectrometer EHS [2]. In order to provide a pure unbiased D^0 sample we concentrate this analysis on the topologically unambiguous and uncontaminated 4-prong neutral decay sample (called V4 in the following).

Results on the hadroproduction and decay properties of charm obtained using a prototype version of EHS (CERN experiment NA16) have already been presented [3]. The present version of EHS (Fig. 1) differs from the NA16 version [4] in several respects:

(a) The vertex detector LEBC provides excellent track information consisting of typically 400 bubbles per track (80/cm) with resolved bubble diameter $\leq$ 20μm in space and excellent contrast. The two track resolution is better than 20 μm and the precision in the measurement of a bubble centre in the film plane is $\sim$ 2 μm. We are sensitive with good efficiency to decay times as short as $\sim 10^{-13}$ s at the film scanning stage.

(b) Angular and momentum precision on charged tracks was considerably improved by including a zeroth lever arm between LEBC and the superconducting magnet M1. This consisted of two high resolution single plane MWPC's W0 (0.5 mm pitch) and W1 (1 mm pitch) and a two-plane inclined wire chamber PIC operated in drift mode with spatial resolution of $\sim$ 100 μm and two track resolution of $\sim$ 300 μm.

(c) Both the first and second lever arms used for momentum analysis are equipped with wire/drift chambers (18 planes in the first lever-arm, 12 in the second). The momentum precision is better than 1% over the entire momentum range.

(*) In this paper the symbol D^0 denotes both D^0 and $\bar{D}^0$ unless explicitly noted otherwise.

(d) Particle identification is provided by ISIS [5] and SAD [6]. ISIS is a large volume drift chamber which measures the ionization of each track with a FWHM resolution of 7%. This allows e-π separation up to 20 GeV/c and π-K separation between 3 and about 50 GeV/c. The silica aerogel Cerenkov detector (SAD) is used for particle identification in the momentum range 0.5 - 4.5 GeV/c. Particle identification is extremely important for the resolution of kinematic ambiguities between charm decay modes.

As for NA16, gamma and electron detection is given by the two lead glass walls, IGD and FGD [7] which are matched to detect with good efficiency the π^0's produced in the forward hemisphere.

To trigger the bubble chamber flash and the spectrometer readout, we use a minimum-bias interaction trigger requiring a multiplicity ≥ 3 in W0 and W1. Under these conditions we record data for off-line analysis corresponding to 85% of the total inelastic cross section, i.e. $\sim$ 17 mb. A total of 265000 good hydrogen interactions were recorded, giving a sensitivity of 15.8 $\pm$ 0.8 events per μb.

Events were double scanned for decay candidates within an area defined in the film plane, centered along the incident particle and extending 2 mm either side of the beam in the transverse direction and over the full length of the chamber along the beam ($\leq$ 11 cm). These limits have a negligible effect on the acceptance of charm particles with decay times less than 6×10^{-12} s and are in any case taken into account for the lifetime determination. They allow the definition of a well defined scanning area for charm. The scanning efficiency for charm topologies in this area with decay length greater than ℓ_{min} (see below) has been estimated to be 95% on the basis of two independent scans followed by a physicist check for charm topologies.

All V4 candidates found in the scanning were measured on a high precision machine (Strasbourg-HPD) which enables us to detect impact

parameters of secondary tracks with respect to the primary vertex down to 7 μm. This precision is essential for a clean definition of the topology of the events. 22 events contain a V4; in 19 of these a second charm vertex is detected. The results reported in this paper are based on these 22 V4 decays.

Table 1 summarizes the main properties of these decays.

In general a four-prong decay can be interpreted in terms of several ambiguous kinematical solutions. We retain for physics analysis only those solutions compatible with the additional information provided by the particle identification system. In most cases this leads to a unique interpretation of the decay. For each charged particle crossing ISIS we compute an ionization probability for the possible mass assignments (electron, pion, kaon). Kinematic solutions corresponding to an ionization probability < 1% for any of the decay products are rejected. The validity of this selection has been confirmed on a sample of 900 strange particle decays and electron pairs [5]. In Table 1 particles with measured ionization consistent with the kinematic interpretation are underlined once and those which are uniquely identified are underlined twice. No ionization information is available for particles not underlined.

Events 1 to 5 of Table 1 are completely reconstructed and give the 3C kinematic fit solutions listed in the table. Events 6 to 9 have one charged particle with no momentum measurement, but yield a four-body 2C kinematic solution. Events 10 to 15 are interpreted in terms of a five-body decay mode, with a π^0 which has been reconstructed for event 10. In general (id = 11,12,14,15) events with an unobserved π^0 give two possible kinematical solutions: in these cases, the two solutions are given in Table 1. Two events have an identified electron (id = 16,17). Event 16 has a 12 GeV/c positive track for which the electron mass assignment is unique: it gives a shower of 12 GeV in IGD and ISIS gives an e/π probability ratio of 50/1. The unambiguous interpretation of this decay is given in Table 1: it is a semileptonic Cabibbo suppressed decay. Event 17 has an electron identified by ISIS but another charged track is outside the spectrometer acceptance and the semileptonic decay hypothesis is underconstrained.

Five events have two or more charged particles not momentum analysed (id = 18 to 22). Most of these particles (labelled 0 in the table) fall outside the spectrometer acceptance. These events are not used for physics analysis.

The visibility weights W_v given in Table 1 take account of the minimum and maximum potential decay lengths for each decay: these lengths have been computed by generating Monte Carlo events using the algorithm described in the NA16 lifetime paper [3b]. One of the decays has a decay length smaller than the computed ℓ_{min} and therefore has a weight equal to zero (id = 13). The average visibility weight is 1.75.

The spectrometer weights W_s given in Table 1 take into account the probability of geometrical acceptance as well as the reconstruction efficiency of decay tracks. Using data on tracks from the primary vertices the reconstruction efficiency in different dip and azimuthal angle bins was determined. Monte Carlo events were generated for the x_F and p_T of each observed event and the probability that at most one charged particle has no measured momentum was estimated. As one can see from the values obtained for these weights, the EHS has an excellent acceptance for the D^0 V4 topology with $x_F > 0$. The average spectrometer weight is 1.1.

Seven experiments contribute to the current world data on the D^0 lifetime, four of them using heavy element targets and detectors, two using high resolution hydrogen bubble chambers, and one from e^+e^- annihilations. The world average lifetime [8] is $\left(4.4 \pm {}^{0.8}_{0.6}\right) \times 10^{-13}$ s but the experiments are very different and often have severe analysis problems so that the spread of the results is due to systematic as well as to statistical errors. In our sample of V4 observed in a hydrogen target, secondary interactions and strange particle decays are topologically excluded, hence there is no background in this D^0 sample.

For the lifetime determination we use the 12 decays which have an unambiguous interpretation. A maximum likelihood analysis applied to these decays yields

$$\tau_{D^0} = 3.5 \begin{matrix} + 1.4 \\ - 0.9 \end{matrix} \times 10^{-13} \text{ s.}$$

Calling t the observed lifetime and t_{min} the minimum detectable one, one finds that the mean $(t-t_{min})$ is smaller than the estimated lifetime by only 6% showing that the maximum potential length correction is small. The stability of the result has been checked as a function of the cuts used to derive visibility weights and no systematic effects can be detected.

In the method described above, the lifetime determination depends on the momentum assigned to each decay. Although we are confident that the decays used in this analysis are identified in a reliable way, we have applied another method [9] which is independent of the kinematics interpretation and therefore uses the entire V4 sample. It makes use of the correlation which exists between the average value of the impact parameters of the decay particles and the lifetime. The experimental value of the average impact parameter is compared to the result of a Monte Carlo analysis which takes into account the scanning efficiency, the measuring precision and the detection probability at the scanning and measuring stage and the experimental x_F and p_T distributions. The resulting lifetime is $\left(3.7 \begin{matrix} + 1.7 \\ - 0.9 \end{matrix} \right) \times 10^{-13}$ s, the errors including both statistical and systematic effects. The consistency of these results with the maximum likelihood analysis increases confidence in the purity of the sample and the value obtained.

To estimate the inclusive D^0 cross section for $x_F > 0$ we consider all the decays with at least three charged tracks well reconstructed in the spectrometer and make use of the visibility and spectrometer weights given in Table 1.

The D^0 into 4 charged particle branching ratio (17 ± 4)% is taken from ref. [10]. Using a scanning efficiency correction factor of 1.05 and an overall experiment sensitivity of 15.8 events/μb, we obtain

$$\sigma(D^0) = (10.3 \pm 3.5)\ \mu b \text{ for } x_F > 0$$

The errors include a contribution due to statistics and to the uncertainty in the V4 branching ratio.

Of the 22 decays, 13 are definitely x_F positive and 6 definitely x_F negative. The forward hemisphere x_F distribution is shown in Fig. 2. As can be seen, the solid line $(1-x_F)^4$ gives a good description of these data. The differential cross section $d\sigma/dx_F$ at $x_F = 0$ is ∿ 50 μb.

The $D^0\pi^+$ and $\bar{D}^0\pi^-$ effective mass spectra (not shown) indicate that four of the 15 decays giving a well defined hadronic final state could be the decay products of the $D^{*\pm}$ (2010), with a background of 0.5 event. The π^0 (and γ) resolution does not permit us to investigate the $D^{0*} \to D^0\pi^0$ and $D^0\gamma$ channels.

To estimate the branching ratio for $D^0 \to K^\pm\pi^\mp\pi^+\pi^-$, we consider the first 17 events of Table 1 with at least three charged tracks reconstructed. Among these events 8 correspond to the four-body decay mode $K^\pm\pi^\mp\pi^+\pi^-$. However, one can show that the 2C fit decays (id = 6 to 9) have a 30% probability to be faked by five-body decays (without changing significantly their total momentum and therefore their lifetime) if their $K^\pm$ is not uniquely identified. Therefore, except for id = 8, we introduce a weight of 0.70 for these decays to estimate the $K^\pm\pi^\mp\pi^+\pi^-$ branching ratio, .

Folding in a V4 branching ratio of (17 ± 4)% we obtain:

$$BR(K^\pm\pi^\mp\pi^+\pi^-) = (7.1 \pm 2.5)\%$$

Note that among these 17 decays, one (id = 4) is a Cabibbo suppressed decay into 4π for which there is no significant fake five-body contamination.

We would like to acknowledge the painstaking work of our scanning and measuring operators, the technical teams involved in the bubble chamber, EHS and SPS operations and the various funding agencies that support the members of our collaboration.

REFERENCES

[1] A. Hervé et al., CERN/82-01 (1982) 69.

[2] W.W.M. Allison et al., CERN/SPSC 76-43 (1976)
G.A. Akopjianov et al., CERN/SPSC 77-44 (1977)
W.W.M. Allison et al., CERN/SPSC 78-91 (1978)
M. Aguilar-Benitez et al., CERN/SPSC 80-50 (1980)
M. Aguilar-Benitez et al., CERN/SPSC 81-86 (1981).

[3] (a) B. Adeva et al., PL 102B (1981) 285
(b) M. Aguilar-Benitez et al., PL 122B (1983) 312
(c) M. Aguilar-Benitez et al., PL 123B (1983) 98
(d) M. Aguilar-Benitez et al., PL 123B (1983) 103
(e) M. Aguilar-Benitez et al., PL 135B (1984) 237

[4] M. Aguilar-Benitez et al., NIM 205 (1983) 79

[5] W.W.M. Allison et al., to be published in NIM (1984).

[6] C. Fernandez et al., to be published in NIM (1984).

[7] B. Powell et al., NIM 198 (1982) 217.

[8] C.G. Wohl et al., Review of particle properties, Rev. Mod. Phys. 56 (1984) S13

[9] P. Checchia et al., Internal INFN/PD/EHS 84 (1984).
S. Petrera, G. Romano, NIM 174 (1980) 61.

[10] G.H. Trilling, Phys. Rep. 75 (1981) 57.

[1] R.W.T.H. Aachen, Germany
[2] Tata Institute of Fundamental Research, Bombay
[3] Vrije Universiteit, Brussels
[4] CERN, European Organization for Nuclear Research, Geneva, Switzerland
[5] Collège de France, Paris, France
[6] Istituto di Fisica, Genova, Italy
[7] University of Chuo, Tokyo, Japan
Metropolitan University, Tokyo, Japan
University of Agriculture and Technology, Tokyo, Japan
University of Hiroshima, Japan
[8] University of Liverpool, United Kingdom
[9] Junta de Eneriga Nuclear, Madrid, Spain
[10] Université de l'Etat, Faculté des Sciences, Mons, Belgium
[11] University of Oxford, Oxford, United Kingdom
[12] University of Padova, Italy
[13] LPNHE, Université Pierre et Marie Curie, Paris, France
[14] University of Rome, Italy
[15] Rutherford Appleton Laboratory, Chilton, United Kingdom
[16] Rutgers University, New Brunswick, U.S.A.
[17] I.H.E.P., Serpukhov, U.S.S.R.
[18] University of Stockholm, Sweden
[19] C.R.N. Strasbourg, France
[20] University of Tennessee, Knoxville, U.S.A.
[21] University of Torino, Italy
[22] University of Trieste, Italy
[23] Institut für Hochenergiephysik, Vienna, Austria

Table 1

r/f	id	ndf	mode	m(Δm) MeV/c2	W_v	W_s	x_F	p_T GeV/c	t 10^{-13}s	$t-t_{min}$ 10^{-13}s
66/1137	1	3	$\underline{K}^-\underline{\underline{\pi}}^+\underline{\pi}^+\underline{\pi}^-$	1865 (4)	2.00	1.37	- 0.02	0.67	14.3	12.8
105/3369	2	3	$\underline{\underline{K}}^-\underline{\pi}^+\underline{\pi}^+\underline{\pi}^-$	1872 (5)	1.85	1.14	0.03	0.97	3.7	1.6
121/4127	3	3	$K^+\underline{\pi}^+\underline{\underline{\pi}}^-\pi^-$	1851 (8)	1.63	1.05	0.11	0.96	5.0	3.6
123/2514	4	3	$\underline{\underline{\pi}}^+\underline{\pi}^+\underline{\underline{\pi}}^-\underline{\pi}^-$	1873 (6)	1.85	1.14	0.03	0.62	2.6	1.7
158/ 828	5	3	$K^-\underline{\underline{\pi}}^+\pi^+\underline{\pi}^-$	1858 (8)	1.52	1.01	0.63	0.66	2.5	1.3
112/ 933	6	2	$\underline{K}^-\underline{\pi}^+\underline{\pi}^-(\pi^+)$		1.48	1.03	0.21	0.67	5.6	3.0
135/2169	7	2	$(K^+)\underline{\underline{\pi}}^+\underline{\pi}^-\underline{\pi}^-$		1.62	1.05	0.12	0.12	2.9	1.2
139/2152	8	2	$\underline{\underline{K}}^+(\pi^+)\pi^-\pi^-$		2.21	2.89	- 0.09	0.73	2.2	0.5
149/3063	9	2	$K^-(\pi^+)\underline{\pi}^+\pi^-$		1.45	1.02	0.39	0.78	5.3	3.5
200/5019	10	3	$\underline{\underline{K}}^-\underline{\underline{\pi}}^+\underline{\pi}^+\underline{\pi}^-\underline{\underline{\pi}}^0$	1870 (14)	1.75	1.41	0.06	0.82	9.5	6.3
32/2775	11	0	$\underline{\underline{K}}^+\underline{\underline{\pi}}^+\underline{\underline{\pi}}^-\underline{\pi}^-(\pi^0)$		1.75	1.39	0.06	0.95	15.2	13.1
					1.50	1.14	0.19	1.94	7.4	6.4
66/4102	12	0	$\underline{\underline{K}}^+\underline{\underline{\pi}}^+\underline{\underline{\pi}}^-\pi^-(\pi^0)$		1.98	2.35	- 0.01	0.72	8.3	4.3
					1.90	1.82	0.02	0.89	6.7	3.5
120/2716	13	0	$\underline{K}^+\underline{\underline{\pi}}^+\underline{\pi}^-\underline{\pi}^-(\pi^0)$		0.0	1.08	0.26	1.47	2.1	- 0.3
133/3220	14	0	$\underline{\underline{K}}^+\underline{\underline{\pi}}^+\underline{\underline{\pi}}^-\underline{\underline{\pi}}^-(\pi^0)$		1.90	1.76	0.02	0.47	16.3	12.5
					1.58	1.18	0.13	0.92	8.3	6.3
134/758	15	0	$K^-\pi^+\pi^+\underline{\pi}^-(\pi^0)$		1.46	1.08	0.24	0.32	3.9	0.9
			$\pi^+\pi^+\pi^-\underline{\pi}^-(K^0)$		1.46	1.08	0.24	0.30	4.0	).9
17/4630	16	0	$\underline{\underline{e}}^+\underline{\pi}^+\underline{\pi}^-\underline{\pi}^-(\nu)$		1.50	1.04	0.20	2.11	0.9	0.1
161/ 345	17		$\underline{\underline{e}}^+ + - 0$							
134/ 559	18		$\underline{\underline{\pi}}^-\underline{\underline{\pi}}^- 00$							
101/1745	19		$++00$							
153/ 596	20		$--00$							
89/1445	21		-000							
94/1018	22		$+000$							

TABLE CAPTION

Main characteristics of the D^0 (V4 topology) observed in this experiment. The table gives for each decay an identification number (id), the number of degrees of freedom of the kinematic fits (ndf), the decay mode, the effective mass with its error (m(Δm)), the visibility and spectrometer weights as explained in the text (W_v, W_s), Feynman-x(x_F), the transverse momentum (p_T), the proper time (t) and the corrected proper time $t-t_{min}$. Unobserved neutral particles or charged particles with no momentum measurement are in brackets. Observed charged particles falling outside the spectrometer acceptance are indicated by the letter O. Particles with measured ionization consistent with the kinematic interpretation are underlined once and those which are uniquely identified are underlined twice. No ionization information is available for particles not underlined.

FIGURE CAPTIONS

1. EHS experimental set-up used in this experiment.

2. $d\sigma/dx_F$ for the 14 $\bar{D}^0$, D^0 produced at positive x_F. The dots represent the actual number of events observed in each bin. The histogram corresponds to the weighted events. The curve represents a cross section of $(1-x_F)^4$ normalized to the weighted number of events.

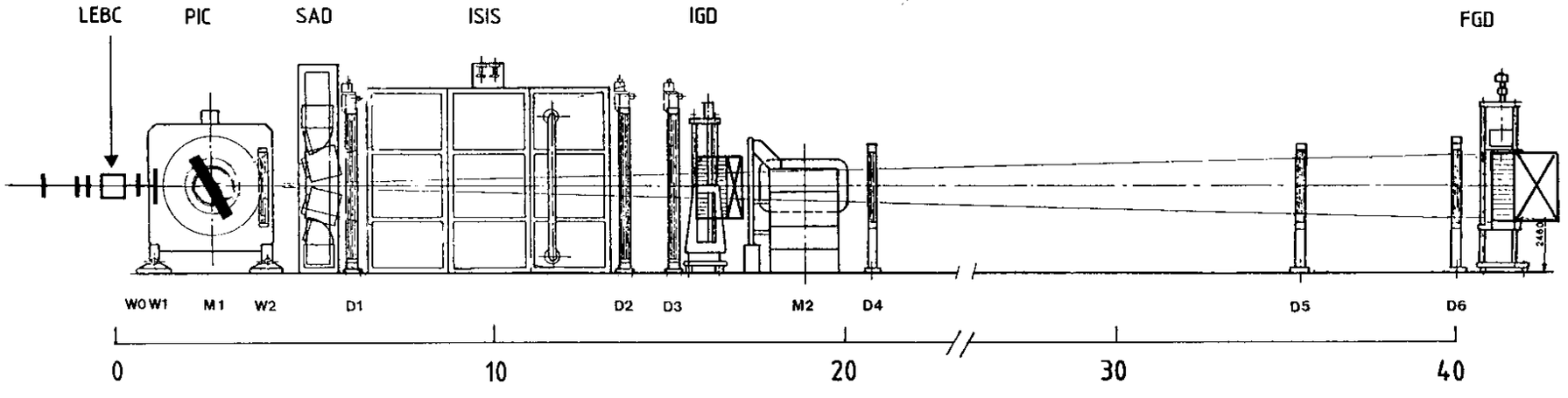
LEBC
PIC
SAD
ISIS
IGD
FGD
W0 W1
M1
W2
D1
D2
D3
M2
D4
D5
D6
0
10
20
30
40

FIG. 1

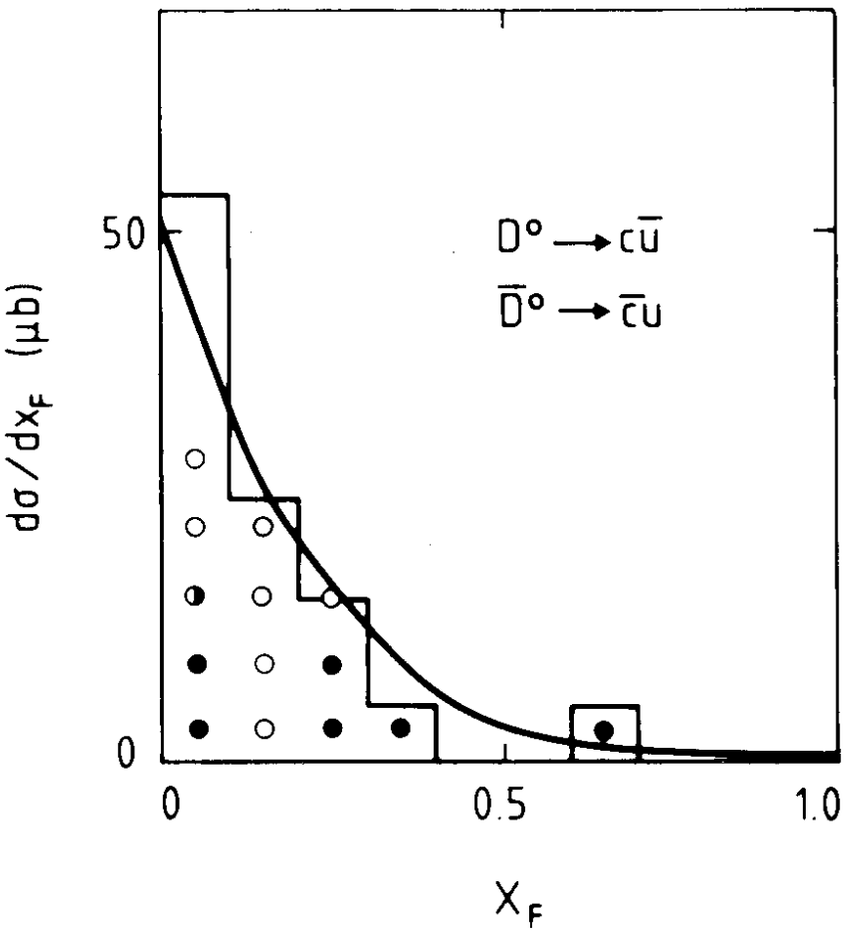
50
0
0
0.5
1.0
$D^0 \rightarrow c\bar{u}$
$\bar{D}^0 \rightarrow \bar{c}u$
$d\sigma/dx_F$ (μb)
X_F

FIG. 2